


# Effects of internal and external decoherence on the resonant transport and Anderson localization of fermionic particles in disordered tight-binding chains

Andrey R. Kolovsky 

*Kirensky Institute of Physics, Federal Research Center KSC SB RAS, 660036 Krasnoyarsk, Russia  
and International Research Center of Spectroscopy and Quantum Chemistry – IRC SQC, Siberian Federal University,  
660041 Krasnoyarsk, Russia*



(Received 26 March 2024; revised 18 June 2024; accepted 20 June 2024; published 8 July 2024)

We study the effects of relaxation/decoherence processes on quantum transport of noninteracting Fermi particles across the disordered tight-binding chain, where we distinguish between relaxation processes in the contacts (external decoherence) and those in the chain (internal decoherence). It is shown that external decoherence reduces conductance fluctuations but does not alter the Anderson localization length. This is in strong contrast with the effect of internal decoherence which is found to suppress Anderson localization. We also address quantum transport in chains with particle losses which are of considerable interest for laboratory experiments with cold atoms.

DOI: [10.1103/PhysRevB.110.035410](https://doi.org/10.1103/PhysRevB.110.035410)

## I. INTRODUCTION

One finds phenomena of resonant transmission in many different physical systems, including the mesoscopic semiconductor devices where the electric current is greatly enhanced for certain values of the gate voltage. The origin of this effect is the enhanced transmission probability for the Bloch wave when its energy coincides with one of the device's eigenenergies. Thus, if we fix the Bloch wave energy to the Fermi energy of electrons in the contacts and change the gate voltage, the transmission probability will show a number of resonant peaks. However, in laboratory experiments one measures not the transmission probability for the Bloch wave but the electric current, where the resonant peaks are broadened. As is known, there are several mechanisms for peak broadening: (i) a finite deference in the chemical potential of the contacts, (ii) a finite temperature, and (iii) quantum decoherence due to relaxation processes which usually present in the system. While the first two mechanisms are well studied, the last one is still under active research [1–4].

In the present work we study the two-terminal transport of noninteracting spinless fermions by using the model of Refs. [5–9] (see the next section) which explicitly takes into account the relaxation process in the contacts. We analyze the resonant transmission in tight-binding chains with and without a disorder. It is shown that dissipative dynamics of the contacts leads to the broadening of the resonant peaks, which appears to be different in disordered chains as compared to the case of no disorder. We mention that the broadening of the resonant peaks implies the carriers transporting states are partially incoherent. In this paper, we refer to this decoherence as external decoherence because its origin is the dissipative dynamics of the contacts.

The diametrically opposed phenomenon to resonant transmission is the Anderson localization in disordered chains. A nice feature of our transport model is its numerical simplicity that allows us to consider long chains needed to address the

Anderson localization. We analyze the effects of both external decoherence and internal decoherence due to relaxation and/or decoherence processes which may be present in the chain. It is shown that internal decoherence strongly affects the critical length of the chain,  $L_{cr}$ , above which the chain is essentially insulating. On the contrary, external decoherence has little effect on the critical length; however, it strongly reduces conductance fluctuations in chains which are shorter than  $L_{cr}$ .

Finally, we address quantum transport in chains with induced particle losses (the “leaky” chains), a problem which is of particular interest for laboratory experiments with cold atoms in optical lattices [10–12], where introducing a controlled disorder is a routine procedure [13,14].

## II. THE MODEL AND THE NUMERICAL METHOD

Following Ref. [9] we consider the tight-binding chain of the length  $L$  connected at both ends to the contacts via the reduced hopping matrix element  $\epsilon \ll J$ . The contacts are modeled by the tight-binding rings of size  $M$ , which eventually tends to infinity, and we include in the model the Lindblad operators which enforce the isolated rings ( $\epsilon = 0$ ) to relax to the thermal equilibrium with the relaxation rate  $\gamma$ . Thus, we have

$$\hat{H} = \hat{H}_s + \sum_{j=1,L} (\hat{H}_{r,j} + \hat{H}_{c,j}). \quad (1)$$

Here, the subindex “s” stands for the chain (the system of interest), the subindex “r” stands for the rings (the reservoirs), the subindex “c” stands for the coupling between the system and the reservoirs, and the indexes  $j = 1$  and  $j = L$  correspond to the left and right reservoirs, respectively. The explicit form of the Hamiltonians in Eq. (1) is the following:

$$\hat{H}_s = \sum_{\ell=1}^L \delta_{\ell} \hat{c}_{\ell}^{\dagger} \hat{c}_{\ell} - \frac{J}{2} \sum_{\ell=1}^{L-1} \hat{c}_{\ell+1}^{\dagger} \hat{c}_{\ell} + \text{H.c.}, \quad (2)$$

$$\widehat{\mathcal{H}}_r = -J \sum_{k=1}^M \cos\left(\frac{2\pi k}{M}\right) \widehat{b}_k^\dagger \widehat{b}_k, \quad (3)$$

$$\widehat{\mathcal{H}}_{c,j} = -\frac{\epsilon}{2} \frac{1}{\sqrt{M}} \sum_{k=1}^M \widehat{c}_j^\dagger \widehat{b}_k + \text{H.c.} \quad (4)$$

Notice that we use the quasimomentum basis for the rings and the Wannier basis for the chain. The governing master equation for the total density matrix  $\mathcal{R}(t)$  reads

$$\frac{\partial \widehat{\mathcal{R}}}{\partial t} = -\frac{i}{\hbar} [\widehat{\mathcal{H}}, \widehat{\mathcal{R}}] + \gamma \sum_{j=1,L} (\widehat{\mathcal{L}}_j^{(g)} + \widehat{\mathcal{L}}_j^{(d)}), \quad (5)$$

where the Lindblad relaxation operators have the forms

$$\widehat{\mathcal{L}}_j^{(d)} = \sum_{k=1}^M \frac{\bar{n}_{k,j} - 1}{2} (\widehat{b}_k^\dagger \widehat{b}_k \widehat{\mathcal{R}} - 2\widehat{b}_k \widehat{\mathcal{R}} \widehat{b}_k^\dagger + \widehat{\mathcal{R}} \widehat{b}_k^\dagger \widehat{b}_k), \quad (6)$$

$$\widehat{\mathcal{L}}_j^{(g)} = -\sum_{k=1}^M \frac{\bar{n}_{k,j}}{2} (\widehat{b}_k \widehat{b}_k^\dagger \widehat{\mathcal{R}} - 2\widehat{b}_k^\dagger \widehat{\mathcal{R}} \widehat{b}_k + \widehat{\mathcal{R}} \widehat{b}_k \widehat{b}_k^\dagger), \quad (7)$$

$$\bar{n}_{k,j} = \frac{1}{e^{-\beta_j [J \cos(2\pi k/M) + \mu_j]} + 1}, \quad (8)$$

with  $\beta_j$  and  $\mu_j$  being the temperature and chemical potentials of the reservoirs. It is easy to see that the introduced model differs from the common two-terminal transport problem by the presence of the Lindblad relaxation operators parametrized by the relaxation constant  $\gamma$ . This model was introduced in Ref. [5] and has been intensively used to analyze quantum transport in different physical systems [6–9].

There are two complementary analytical approaches to take into account a finite relaxation rate  $\gamma$ . The first one made up of nonequilibrium Green's functions methods and the Keldysh formalism [15–19], which can be viewed as further development of the Landauer-Büttiker theory [20–22]. In particular, in Ref. [7] the authors explicitly include the parameter  $\gamma$  in the lesser Green's function and then follow the standard procedure [22] to calculate the stationary current across the chain. Because for these methods  $\gamma$  is a kind of perturbation to the Landauer theory, they are well suited for a small  $\gamma$ .

The second approach stays with the master equation formalism and it is more suited for a large  $\gamma$ . Here one employs the Born-Markov approximation [23] to eliminate reservoirs and obtain the master equation for the density matrix of the carriers in the chain. This Markovian master equation is known in physical literature as open or boundary driven Hubbard models [24], which often have analytical solutions [26–29]. In our recent works [30,31], we relaxed the Markov approximation and derived the non-Markovian master equation [32] which was demonstrated to recover the Landauer result in the limits  $M \rightarrow \infty$  and  $\gamma \rightarrow \infty$ , where the limit  $M \rightarrow \infty$  should be taken first [33]. In what follows, however, we employ neither of the above discussed analytical approaches but use the pure numerical method to calculate the conductance of a disordered chain for a moderate  $\gamma$ . We discuss the details of this method in the next paragraph.

Since we consider the case of noninteracting fermions, we can obtain from the master equation (5) the equation for the single-particle density matrix (SPDM) in the closed form. We

have

$$\frac{d\rho}{dt} = -i[H, \rho] - G * \rho + \gamma \rho_0. \quad (9)$$

In this equation  $\rho$  is the SPDM of the size  $(M + L + M) \times (M + L + M)$ ,  $H$  is the single-particle version of the many-body Hamiltonian (1),  $\rho_0$  is the diagonal matrix with elements determined by the Fermi distribution (8),  $G$  is the relaxation matrix with elements proportional to  $\gamma$ ,

$$G_{n,m} = \begin{cases} 0, & (n, m) \in L \times L, \\ \gamma, & (n, m) \in M \times M, \\ \gamma/2, & (n, m) \in L \times M, M \times L, \end{cases} \quad (10)$$

and the sign “\*” denotes the element-by-element product of two matrices [34]. Here we use an ordering of the density matrix elements where the corner blocks of the size  $M \times M$  are the contact SPDMs and the central block of the size  $L \times L$  is the chain SPDM. It is easy to see from Eqs. (9) and (10) that for  $\epsilon = 0$  the contacts relax to the thermal equilibrium and, simultaneously, any correlations between the chain and the contacts (i.e., the system and the reservoirs) decay to zero.

We are interested in the nonequilibrium steady-state for  $\epsilon \neq 0$ , which obviously obeys the following algebraic equation:

$$i[H, \rho] + G * \rho = \gamma \rho_0. \quad (11)$$

We solve the algebraic Eq. (11) numerically for a finite ring size  $M$  and watch convergence of the limit  $M \rightarrow \infty$  by comparing  $\rho_s$  (the central block of the total SPDM) calculated for different values of  $M$ . The empirical rule is that  $M$  should be larger than  $1/\gamma$  to get the convergence. Knowing  $\rho_s$  with the desired accuracy, we then calculate the stationary current  $j$  across the chain as

$$j = \frac{1}{L-1} \text{Tr}[\hat{j} \rho_s] \quad (12)$$

(here  $\hat{j}$  is the two-diagonal matrix of the single-particle current operator) and the system conductance as

$$\sigma = \lim_{\Delta\mu \rightarrow 0} \frac{j(\Delta\mu)}{\Delta\mu}, \quad (13)$$

where  $\Delta\mu = \mu_1 - \mu_L$  is the chemical potential difference between reservoirs. We also find it convenient to incorporate the latter limit in the limit  $M \rightarrow \infty$ . In other words, we proportionally decrease  $\Delta\mu$  when increasing the ring size  $M$ .

In what follows, for the sake of simplicity, we assume zero temperatures of the contacts. As the control parameter we choose the gate voltage  $\delta$  which modifies the on-site energies  $\delta_\ell$  in the Hamiltonian (2) as  $\delta_\ell \rightarrow \delta + \xi_\ell$ . (For chains without disorder,  $\xi_\ell = 0$ .) Also, from now on, we use dimensionless parameters where the hopping matrix element  $J$  is the energy unit. Thus,  $\epsilon = 0.1$  or  $\gamma = 0.1$  implies that the coupling constant and the relaxation rate times the Planck constant are one tenth of the hopping energy.

### III. RESONANT TRANSMISSION AND ANDERSON LOCALIZATION

The numerical analysis of the system conductance on the basis of the algebraic equation (11) reveals two asymptotic

results which agree very well with analytical estimates. Namely, in the limit  $\gamma \rightarrow 0$  the conductance is given by the Landauer formula

$$\sigma(\delta) = \frac{1}{2\pi} |t(\delta)|^2, \quad (14)$$

where  $1/2\pi$  is the conductance quantum  $e^2/h$  in our dimensionless units and  $|t(\delta)|^2$  is the transmission probability, which one finds by solving the scattering problem for the Bloch wave. Equation (14) can be elaborated further by assuming the weak-coupling limit  $\epsilon \ll 1$ . Then we have

$$\sigma(\delta) \approx \frac{1}{2\pi} \sum_{n=1}^L \frac{\Gamma_n^2}{\Gamma_n^2 + (\delta - E_n)^2}, \quad \Gamma_n = \frac{\alpha_n \epsilon^2}{2}, \quad (15)$$

where  $E_n$  are the eigenvalues of the isolated chain and  $\alpha_n$  are determined by the eigenfunctions  $\psi_n$  of the isolated chain as

$$\alpha_n = |\langle \psi_n | \langle \ell = 1 \rangle \langle \ell = L | \psi_n \rangle|. \quad (16)$$

We notice that in the original parameters the widths  $\Gamma_n$  are  $\Gamma_n = 0.5\alpha_n \epsilon^2/J$  and, thus, have the dimension of the energy. Also, it is easier to prove that, in the case  $\xi_l = 0$  (no disorder),  $\sum_n \alpha_n = 1$ . It follows from the displayed equation that the widths of conductance peaks are proportional to  $\epsilon^2$  and all peaks have the same height,  $1/2\pi$ .

In the opposite limit of large  $\gamma$  the widths of conductance peaks are determined by the parameter  $\gamma$  while the peak heights are proportional to  $\epsilon^2$ ,

$$\sigma(\delta) \approx \frac{\epsilon^2}{4\pi} \sum_{n=1}^L \alpha_n \frac{(\gamma/2)}{(\gamma/2)^2 + (\delta - E_n)^2}. \quad (17)$$

Notice that the estimate (17) is obtained under the assumption  $\epsilon^2 \ll \gamma$  and, hence, the peak heights are always smaller than  $1/2\pi$ . Equations (17) and (14) can be combined into the following single equation,

$$\sigma(\delta) \approx \frac{1}{2\pi} \sum_{n=1}^L \frac{\Gamma_n(\Gamma_n + \gamma/2)}{(\Gamma_n + \gamma/2)^2 + (\delta - E_n)^2}, \quad (18)$$

which interpolates between the limits  $\gamma \ll \epsilon^2$  and  $\gamma \gg \epsilon^2$ . From the side of the Landauer theory, this equation can be interpreted as the broadening of resonant peaks due to partial decoherence of the carrier transporting states in the chain caused by the contact dissipative dynamics [33].

We compared the estimate (18) with the exact numerical results for different chain lengths  $L$  and, in the case of no disorder, found an excellent agreement. As two examples, Figs. 1(a) and 1(b) show the conductance of the chain  $L = 25$  for  $\gamma = 0.05$ , where the resonant peaks are partially resolved, and  $\gamma = 0.2$ , where peaks merge together resulting in a smooth curve  $\sigma = \sigma(\delta)$  which is insensitive to further increase of the chain length  $L$ .

We come to the second topic of the work. To address the Anderson localization we consider long chains up to  $L = 400$  and introduce random on-site energies, i.e.,

$$\delta_\ell = \delta + \xi_\ell, \quad (19)$$

where  $\xi_\ell$  are uniformly distributed in the interval  $|\xi_\ell| \leq \xi$ . As the reference point we take the chain of the length

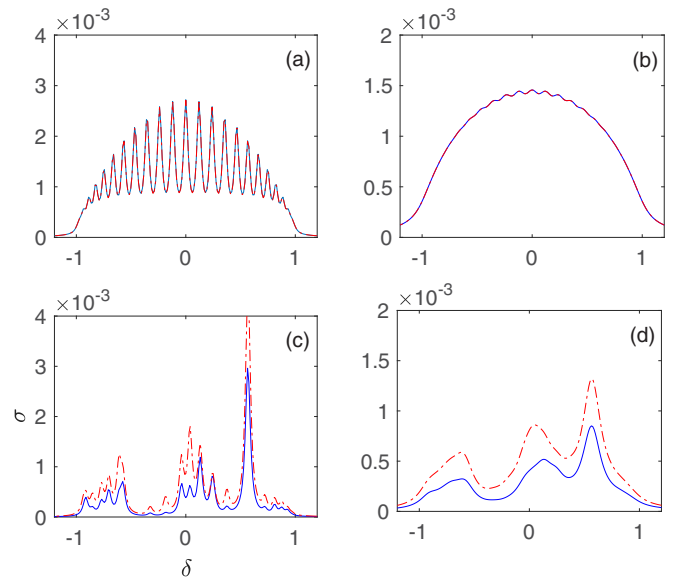


FIG. 1. Conductance of the chain  $L = 25$  for  $\gamma = 0.05$ , left column, and  $\gamma = 0.2$ , right column. The other parameters are  $\epsilon = 0.1$ ,  $\mu = 0$ , and the disorder strength  $\xi = 0$ , upper row, and  $\xi = 0.4$  (a single realization), lower row. The dash-dotted lines are Eq. (18).

$L = 25$  whose conductance for  $\xi = 0$  is depicted in Figs. 1(a) and 1(b). Remarkably, for disordered chains, Eq. (18) does not work as well as for chains without disorder [see Figs. 1(c) and 1(d)]. However, on the qualitative level, it correctly captures all the critical effects of the Anderson localization theory. In particular, it follows from the latter theory that the coefficients  $\alpha_n$ , Eq. (16), are exponentially small if the chain length exceeds the Anderson localization length  $L_A = L_A(\xi)$ . Thus, conductance should also be exponentially small for  $L > L_A$ . The straightforward numerical analysis of the chain conductance in the presence of disorder fully confirms this expectation; see Fig. 2, where the solid lines can be well

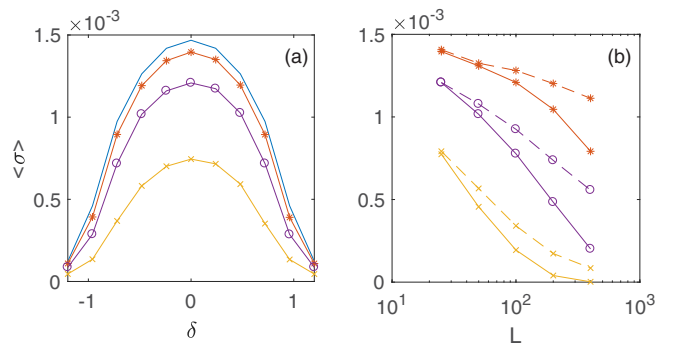


FIG. 2. (a) The average conductance  $\langle \sigma \rangle$  of the chain of the length  $L = 25$  for  $\gamma = 0.2$  and different disorder strengths  $\xi = 0, 0.1, 0.2$ , and  $0.4$ . (b) The average conductance at  $\delta = 0$  as a function of the chain lengths  $L = 25, 50, 100, 200$ , and  $400$  for different disorder strengths  $\xi = 0.1, 0.2$ , and  $0.4$ . Average over 1000 realizations of random on-site energies  $\xi_\ell$ . Additional dashed lines refer to the case of incoherent transport which is discussed later on in Sec. IV.

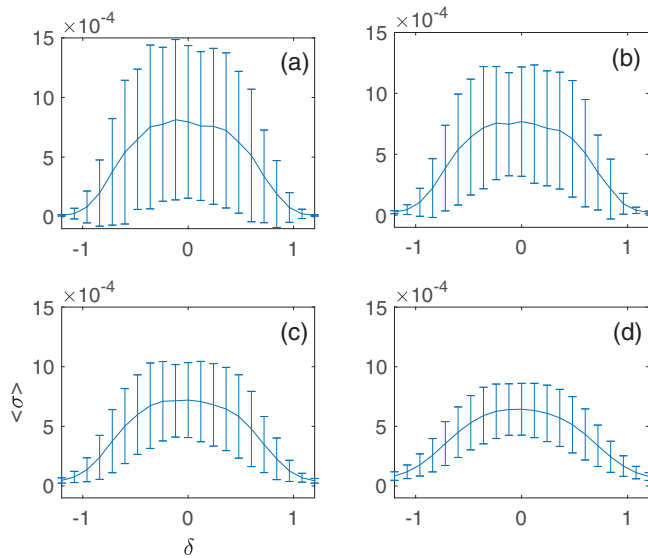


FIG. 3. The average conductance of the chain  $L = 25$  for  $\xi = 0.4$  and different  $\gamma = 0.05$  (a),  $0.1$  (b),  $0.2$  (c), and  $0.4$  (d). (The other parameters are the same as those in Fig. 2.) The lengths of the error bars correspond to standard deviations from the mean values.

approximated by the exponential dependence

$$\sigma \sim \exp(-L/L_{\text{cr}}). \quad (20)$$

In Eq. (20) we introduce the notion of the critical length  $L_{\text{cr}}$  to stress that in the presence of external decoherence  $L_{\text{cr}}$  may deviate from  $L_A$ .

We did preliminary studies of the effect of a finite  $\gamma$  on the Anderson localization. It was found that an increase or decrease of  $\gamma$  practically does not affect the critical chain length  $L_{\text{cr}}$  above which it becomes insulating. However, an increase or decrease of  $\gamma$  strongly decreases or increases fluctuations of the function  $\sigma = \sigma(\delta)$  (see Fig. 3). Thus, by measuring conductance fluctuations in a laboratory experiment one can extract the value of the relaxation constant  $\gamma$ .

#### IV. DISSIPATIVE LATTICES

In this section we discuss the dissipative lattices which are of particular interest for quantum transport of cold atoms in optical lattice with induced particle losses [10–12]. In the general case these losses are described by the Lindblad operator

$$\hat{\mathcal{L}}_{\text{loss}} = \sum_{\ell=1}^L \frac{\tilde{\gamma}_{\ell}}{2} (\hat{c}_{\ell}^{\dagger} \hat{c}_{\ell} \hat{\mathcal{R}} - 2\hat{c}_{\ell} \hat{\mathcal{R}} \hat{c}_{\ell}^{\dagger} + \hat{\mathcal{R}} \hat{c}_{\ell}^{\dagger} \hat{c}_{\ell}), \quad (21)$$

where  $\gamma_{\ell}$  is the loss rate at a given lattice site. Playing with constants  $\gamma_{\ell}$  one can address different physical situations, for example, to mimic ionizing an electron beam of a given width. The limiting case where all  $\gamma_{\ell}$  except for  $\ell = \ell_0$  were zero was analyzed in Refs. [2,4] by using the Keldysh formalism. Here we consider the opposite situation where all constants are the same,  $\gamma_{\ell} = \tilde{\gamma}$ .

It is easy to show that adding the Lindblad operator (21) to the master equation (5) redefines the relaxation matrix in

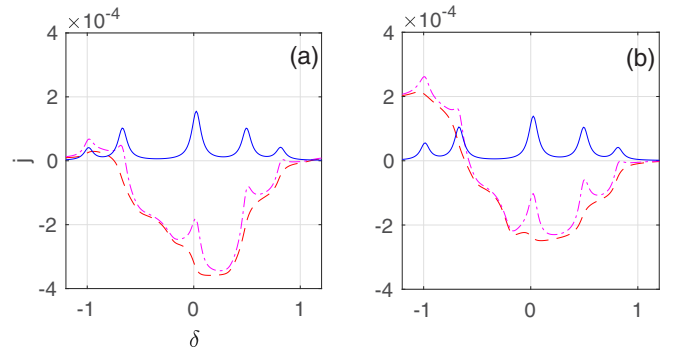


FIG. 4. The current Eq. (12) as the function of the gate voltage  $\delta$  for the model (23), panel (a), and the model (22), panel (b). The system parameters are  $L = 5$ ,  $\xi = 0.4$ ,  $\gamma = 0.1$ ,  $\tilde{\gamma} = 0.001$ , and  $\Delta\mu = 0$  (red dashed lines) and  $\Delta\mu = \pi/160$  (magenta dash-dotted lines). The blue solid lines are the net current given by the difference between dash-dotted and dashed lines.

Eqs. (9) and (11) as  $G \rightarrow G + \tilde{G}$ , where

$$\tilde{G}_{n,m} = \begin{cases} \tilde{\gamma}, & (n, m) \in L \times L. \\ 0, & (n, m) \in M \times M, \\ \tilde{\gamma}/2, & (n, m) \in L \times M, M \times L. \end{cases} \quad (22)$$

Thus, if we assume for a moment  $\epsilon = 0$ , the chain density matrix  $\rho_s(t)$  decays to zero. Commonly, the decay of off-diagonal elements of a density matrix is referred to as quantum decoherence while the decay of diagonal elements is referred to as dissipation. It is instructive to consider these two processes separately. We begin with the quantum decoherence without dissipation or losses where the matrix  $\tilde{G}$  has the form

$$\tilde{G}_{n,m} = \begin{cases} \tilde{\gamma}(1 - \delta_{n,m}), & (n, m) \in L \times L, \\ 0, & (n, m) \in M \times M, \\ \tilde{\gamma}/2, & (n, m) \in L \times M, M \times L. \end{cases} \quad (23)$$

We mention that this form of the relaxation matrix mimics to some extent the decoherence effect of the phonon subsystem in solid-state devices. To distinguish this decoherence from the decoherence effect of the contacts, we use the term internal decoherence.

A remarkable consequence of internal decoherence is that (among the other effects [38]) it can lead to the ratchet effect [39–41] where the system with broken spatial symmetry shows directed current even in the absence of chemical potential difference. Clearly, the ratchet current is sensitive to a particular realization of the on-site disorder  $\xi_{\ell}$  and it is strictly zero for chains without disorder. As an example, the red dashed line in Fig. 4(a) shows the ratchet current in the chain of the length  $L = 5$  for  $\Delta\mu = 0$  and the disorder strength  $\xi = 0.4$ . For this particular realization of disorder the current is seen to be negative for almost all  $\delta$ , but for other realizations it can be positive or alternating between positive and negative values. In the case  $\Delta\mu \neq 0$  the ratchet current gives a background for the total current, which is depicted by the dashed-dotted magenta line. Taking the difference between the total and ratchet currents we get the net current, see the solid blue line in Fig. 4(a). We found that for  $\tilde{\gamma} \ll \gamma$  the net current almost coincides with the current between the contacts

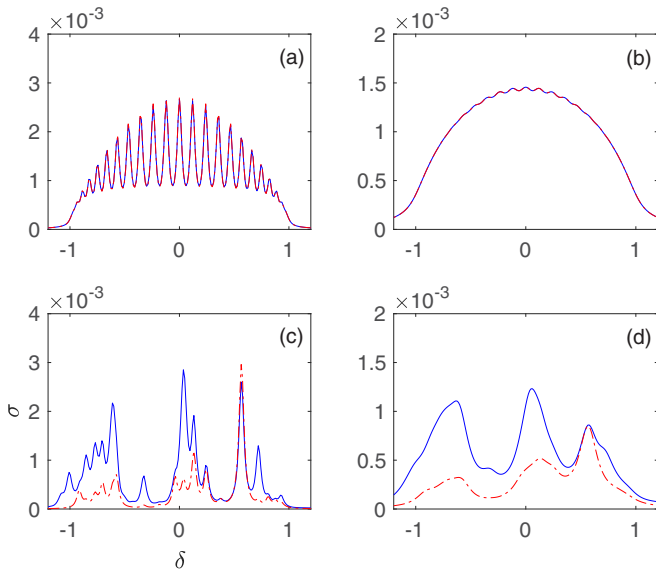


FIG. 5. The same as in Fig. 1 yet in the presence of a weak internal decoherence with the rate  $\tilde{\gamma} = 0.001$ . The dot-dashed lines copy the solid lines from Fig. 1.

in the absence of internal decoherence. Yet, there are some deviations which become more apparent for longer lattices. Thus, the next question to address is the Anderson localization in the presence of internal decoherence.

### A. Anderson localization

Since the Anderson localization is a coherent phenomenon, one may expect internal decoherence to destroy it. We check this hypothesis by repeating the analysis of Sec. III for the relaxation matrix  $G$  in Eq. (11) given by the sum of the matrix (10) and the matrix (23). As the reference point we again choose the lattice of the length  $L = 25$  and restrict ourselves by the case  $\tilde{\gamma} \ll \gamma$ . For  $\tilde{\gamma} = 0.001$  and the other parameters as given in Fig. 1, the system conductance Eq. (13), where  $j = j(\delta, \Delta\mu)$  is now the *net current*, is depicted in Fig. 5. It is seen that a weak decoherence indeed enhances the conductance of the disordered chain, leaving the conductance of the perfect ( $\xi = 0$ ) chain the same.

The conductance averaged over different realizations of the on-site disorder is shown in Fig. 6. Notice that for the average conductance we do not need to decompose the total current into the net and ratchet currents because the latter self-averages to zero. Comparing the results depicted in Fig. 6 with those depicted in Fig. 2, we conclude that a weak internal decoherence strongly suppresses the Anderson localization. Functional dependence of the critical chain length  $L_{\text{cr}}(\xi)$  (i.e., the length below which the disordered chain is conducting) on the decoherence rate  $\tilde{\gamma}$  remains an open problem.

### B. Leaky chains

Now we include dissipation into the analysis, i.e., switch back to the original problem of Eqs. (21) and (22). For this model and the chain  $L = 5$  the total and net currents are shown in Fig. 4(b). Having quite a similar result as for the previous model, one might naively conclude that the model Eq. (22)

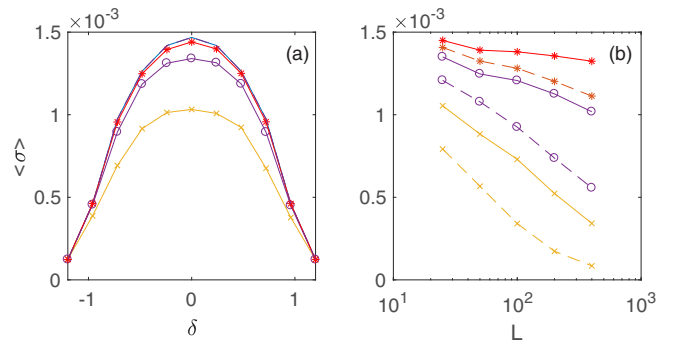


FIG. 6. The same as in Fig. 2 yet in the presence of a weak internal decoherence  $\tilde{\gamma} = 0.001$ . The dashed lines in panel (b) and in Fig. 2(b) show the result for even smaller  $\tilde{\gamma} = 0.0001$ .

does not require a separate consideration. This is, however, not the case because, unlike for the model Eq. (23), the mean current Eq. (12) is now unrelated to the current between the contacts. Indeed, assuming for a moment  $\Delta\mu = 0$ , particles from both contacts go into the chain where they are lost. Thus, instead of Eq. (12), one should consider the particle loss current

$$j_{\text{loss}} = \tilde{\gamma} \text{Tr}[\rho_s], \quad (24)$$

which coincides with the sum of currents flowing from the left and right contacts.

As an example, Fig. 7(a) shows these three currents for  $\Delta\mu = 0$  and the chain length  $L = 5$ . Notice that for a disordered chain the particle flow from the left and right contacts are different and they coincide only if  $\xi = 0$ . We also mention that the leakage current is restricted from above by the value  $\tilde{\gamma}L$  because for the Fermi particles  $\text{Tr}[\rho_s] \leq L$ .

Figure 7(b) shows the discussed three currents in the case  $\Delta\mu \neq 0$ . At first glance, the depicted dependencies are structureless. Yet, they carry important information which is revealed by taking the difference between the corresponding curves in the two panels [see Fig. 8(b)]. [For the sake of completeness, we also depict in Fig. 8(a) the result for  $\xi = 0$ .] The revealed peaklike structure of the net current is obviously a signature of the resonant transmission. Since in laboratory

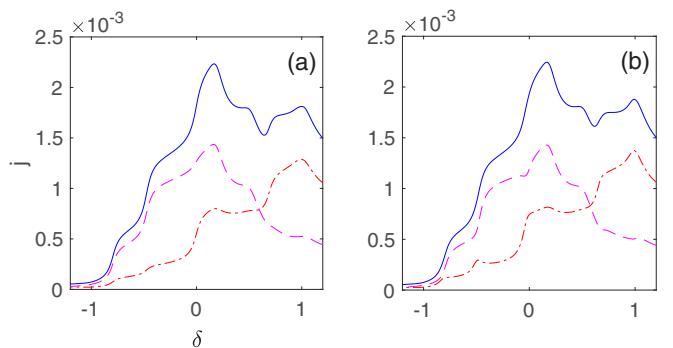


FIG. 7. The currents between the chain and the contacts (dashed and dash-dotted lines) and the particle loss current (solid line) in the dissipative disordered chain. The system parameters are  $L = 5$ ,  $\xi = 0.4$ ,  $\gamma = 0.1$ ,  $\tilde{\gamma} = 0.001$ ,  $\mu = 0$ , and  $\Delta\mu = 0$  (a) and  $\Delta\mu = \pi/160$  (b).

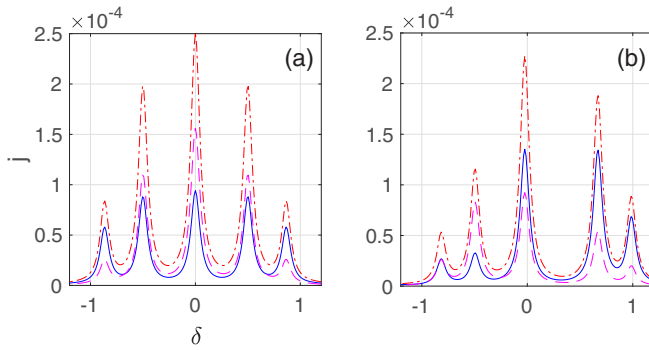


FIG. 8. The difference between the corresponding curves in Fig. 7. Panels (a) and (b) refer to the cases  $\xi = 0$  and  $\xi = 0.4$ , respectively.

experiments with neutral atoms the number of lost particles can be measured with very high accuracy, this opens new perspectives in studying the resonant transmission.

Finally, we discuss the signature of the Anderson localization in leaky chains. Figure 9 compares occupation numbers  $n_\ell$  of the chain without disorder (red dashed line) with those of the disordered chain (blue solid lines) for  $\tilde{\gamma} = 0.0001$  and the coupling constant  $\epsilon = 0.1$ . In the first case, since the hopping rate  $J = 1$  in the chain is much larger than the hopping rate  $\epsilon$  and the depletion rate  $\tilde{\gamma}$ , the chain population is almost flat. In the second case, due to the presence of disorder, we observe an exponential decrease of population towards the chain centrum,  $n_\ell \sim \exp(-\ell/L_\gamma)$ , where  $L_\gamma$  is determined by an interplay among the coherent Anderson localization length  $L_A$ , the decoherence rate  $\tilde{\gamma}$ , and the depletion rate which, within the framework of the considered model, coincides with the decoherence rate.

## V. CONCLUSION

We revisit the problem of two-terminal transport of non-interacting Fermi particles across the tight-binding chain by using the master equation formalism. We analyze the effects of decoherence processes in the chain (internal decoherence with the rate  $\tilde{\gamma}$ ) and relaxation processes in the contacts (external decoherence with the rate  $\gamma$ ) on conductance of the perfect (i.e., without disorder) and disordered chains of arbitrary length  $L$ . It is shown that external decoherence leads to

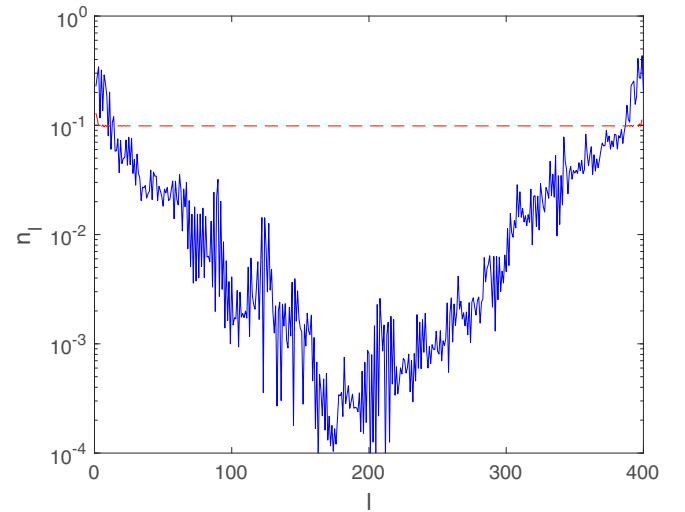


FIG. 9. Occupation numbers  $n_\ell$  of the perfect (red dashed line) and disordered (blue solid line) leaky chains. Parameters are  $\epsilon = 0.1$ ,  $\gamma = 0.2$ ,  $\tilde{\gamma} = 0.0001$ , and  $\xi = 0.4$ .

the broadening of resonant peaks but does not affect the integrated conductance of perfect chains. As concerns disordered chains, external decoherence reduces conduction fluctuations but does not alter the critical length  $L_{cr}$  above which the chain is insulating.

The effect of internal decoherence is more subtle. In the work we restricted ourselves by the case  $\tilde{\gamma} \ll \gamma$  where the contribution of internal decoherence into the widths of resonant peaks and conductance fluctuations is negligible. Yet, it is found that this weak internal decoherence strongly affects the critical length  $L_{cr}$  as compared to the Anderson localization theory.

We also consider situations where internal decoherence is accompanied by particle losses. In this case the main quantity to study is the leakage current, the number of particles which are lost in the chain per time unit. It is demonstrated that the phenomena of resonant transmission and Anderson localization are well reflected in the leakage current.

## ACKNOWLEDGMENT

This study was supported by the Ministry of Science and Higher Education of Russian Federation, Grant No. FSRZ-2023-0006.

- 
- [1] T. Jin, M. Filippone, and T. Giamarchi, Generic transport formula for a system driven by Markovian reservoirs, *Phys. Rev. B* **102**, 205131 (2020).
  - [2] A.-M. Visuri, T. Giamarchi, and C. Kollath, Symmetry-protected transport through a lattice with a local particle loss, *Phys. Rev. Lett.* **129**, 056802 (2022).
  - [3] S. Uchino, Comparative study for two-terminal transport through a leaky one-dimensional quantum wire, *Phys. Rev. A* **106**, 053320 (2022).
  - [4] A.-M. Visuri, T. Giamarchi, and C. Kollath, Nonlinear transport in the presence of a local dissipation, *Phys. Rev. Res.* **5**, 013195 (2023).
  - [5] S. Ajisaka, F. Barra, C. Mejía-Monasterio, and T. Prosen, Nonequilibrium particle and energy currents in quantum chains connected to mesoscopic Fermi reservoirs, *Phys. Rev. B* **86**, 125111 (2012).
  - [6] S. Ajisaka and F. Barra, Nonequilibrium mesoscopic Fermi-reservoir distribution and particle current through a coherent quantum system, *Phys. Rev. B* **87**, 195114 (2013).

- [7] D. Gruss, K. A. Velizhanin, and M. Zwolak, Landauer's formula with finite-time relaxation: Kramer's crossover in electronic transport, *Sci. Rep.* **6**, 24514 (2016).
- [8] J. E. Elenewski, D. Gruss, and M. Zwolak, Master equations for electron transport: The limits of the Markovian limit, *J. Chem. Phys.* **147**, 151101 (2017).
- [9] A. R. Kolovsky, Open Fermi-Hubbard model: Landauer's versus master equation approaches, *Phys. Rev. B* **102**, 174310 (2020).
- [10] G. Barontini, R. Labouvie, F. Stubenrauch, A. Vogler, V. Guarrera, and H. Ott, Controlling the dynamics of an open many-body quantum system with localized dissipation, *Phys. Rev. Lett.* **110**, 035302 (2013).
- [11] S. Krinner, T. Esslinger, and J.-P. Brantut, Two-terminal transport measurements with cold atoms, *J. Phys.: Condens. Matter* **29**, 343003 (2017).
- [12] L. Corman, P. Fabritius, S. Häusler, J. Mohan, L. H. Dogra, D. Husmann, M. Lebrat, and T. Esslinger, Quantized conductance through a dissipative atomic point contact, *Phys. Rev. A* **100**, 053605 (2019).
- [13] J. Billy, V. Josse, Z. Zuo, A. Bernard, B. Hambrecht, P. Lugan, D. Clement, L. Sanchez-Palencia, Ph. Bouyer, and A. Aspect, Direct observation of Anderson localization of matter-waves in a controlled disorder, *Nature (London)* **453**, 891 (2008).
- [14] G. Roati, C. D'Errico, L. Fallani, M. Fattori, C. Fort, M. Zaccanti, G. Modugno, M. Modugno, and M. Inguscio, Anderson localization of a non-interacting Bose-Einstein condensate, *Nature (London)* **453**, 895 (2008).
- [15] Y. Meir and N. S. Wingreen, Landauer formula for the current through an interacting electron region, *Phys. Rev. Lett.* **68**, 2512 (1992).
- [16] J. Rammer, *Quantum Field Theory of Non-equilibrium States* (Cambridge University, Cambridge, England, 2007).
- [17] H. Haug, A.-P. Jauho *et al.*, *Quantum Kinetics in Transport and Optics of Semiconductors* (Springer, Berlin, 2008).
- [18] A. Kamenev, *Field Theory of Non-equilibrium Systems* (Cambridge University, Cambridge, England, 2011).
- [19] L. M. Sieberer, M. Buchhold, and S. Diehl, Keldysh field theory for driven open quantum systems, *Rep. Prog. Phys.* **79**, 096001 (2016).
- [20] R. Landauer, Spatial variation of currents and fields due to localized scatterers in metallic conduction, *IBM J. Res. Dev.* **1**, 223 (1957).
- [21] M. Büttiker, Y. Imry, R. Landauer, and S. Pinhas, Generalized many-channel conductance formula with application to small rings, *Phys. Rev. B* **31**, 6207 (1985).
- [22] S. Datta, *Electronic Transport in Mesoscopic Systems* (Cambridge University, Cambridge, England, 1995).
- [23] A. R. Kolovsky, Quantum entanglement and the Born-Markov approximation for an open quantum system, *Phys. Rev. E* **101**, 062116 (2020).
- [24] We mention, in passing, that the considered model is also discussed with respect to bosonic carriers. To address this case one should exchange minus and plus signs in Eq. (6) and use the Bose-Einstein distribution instead of the Fermi-Dirac distribution, Eq. (8) (see Ref. [25], for example).
- [25] P. S. Muraev, D. N. Maksimov, and A. R. Kolovsky, Resonant transport of bosonic carriers through a quantum device, *Phys. Rev. A* **105**, 013307 (2022).
- [26] T. Prosen, Exact nonequilibrium steady state of an open Hubbard chain, *Phys. Rev. Lett.* **112**, 030603 (2014).
- [27] G. Kordas, D. Witthaut, and S. Wimberger, Non-equilibrium dynamics in dissipative Bose-Hubbard chains, *Ann. Phys. (Berlin)* **527**, 619 (2015).
- [28] A. R. Kolovsky, Z. Denis, and S. Wimberger, Landauer-Büttiker equation for bosonic carriers, *Phys. Rev. A* **98**, 043623 (2018).
- [29] G. T. Landi, D. Poletti, and G. Schaller, Nonequilibrium boundary-driven quantum systems: Models, methods, and properties, *Rev. Mod. Phys.* **94**, 045006 (2022).
- [30] A. R. Kolovsky and D. N. Maksimov, Resonant transmission of fermionic carriers: Comparison between solid-state physics and quantum optics approaches, *Phys. Rev. B* **104**, 115115 (2021).
- [31] D. N. Maksimov, S. V. Aksenov, and A. R. Kolovsky, Non-Markovian master equation for quantum transport of fermionic carriers, *J. Phys.: Condens. Matter* **36**, 045301 (2024).
- [32] To avoid a mismatch with Refs. [7,8], it should be mentioned that we use the terms Markovian and non-Markovian with respect to the master equation for the system of interest, where the Markovian and non-Markovian regimes are opposite to those shown in Fig. 2(a) in Ref. [8].
- [33] A. R. Kolovsky, Deriving Landauer's result by using the master equation approach, *Europhys. Lett.* (2024) (to be published)
- [34] We mention Refs. [35–37] where Eqs. (9) and (10) were introduced and analyzed in some detail without referring the many-body Hamiltonian (1).
- [35] T. Zelovich, L. Kronik, and O. Hod, State representation approach for atomistic time-dependent transport calculations in molecular junctions, *J. Chem. Theory Comput.* **10**, 2927 (2014).
- [36] O. Hod, C. A. Rodriguez-Rosario, T. Zelovich, and T. Frauenheim, The driven Liouville von Neumann equation in Lindblad form, *J. Phys. Chem. A* **120**, 3278 (2016).
- [37] T. Zelovich, L. Kronik, and O. Hod, Driven Liouville von Neumann approach for time-dependent electronic transport calculations in a nonorthogonal basis-set representation, *J. Phys. Chem. C* **120**, 15052 (2016).
- [38] E. Zerah-Harush and Y. Dubi, Effects of disorder and interactions in environment assisted quantum transport, *Phys. Rev. Res.* **2**, 023294 (2020).
- [39] P. Reimann, M. Grifoni, and P. Hänggi, Quantum ratchets, *Phys. Rev. Lett.* **79**, 10 (1997).
- [40] J. Peguiron and M. Grifoni, Duality relation for quantum ratchets, *Phys. Rev. E* **71**, 010101(R) (2005).
- [41] K. Hamamoto, T. Park, H. Ishizuka, and N. Nagaosa, Scaling theory of a quantum ratchet, *Phys. Rev. B* **99**, 064307 (2019).